Prediction of the Voltage Drop due to the Diode Commutation Process in the Excitation System of Salient-Pole Synchronous Generators

S. Nuzzo*, M. Galea*, C. Gerada*, and N. L. Brown**
* Power Electronics, Machine Drives and Control Group, University Of Nottingham, UK
** Research and Technology Department, Cummins Power Generation, Peterborough, UK

***Abstract*--The commutation processes in uncontrolled diode rectifiers have been extensively studied and modelled. However, in some applications, such as electrical power generation, the effects of these processes are often neglected. In low to medium rated, field wound, synchronous generators, the excitation system makes up a significant percentage of the whole generating set. Thus, the voltage drop due to the diode commutations can be quite significant. It is therefore of critical importance that these are considered during all the design stages of the brushless excitation system of synchronous generators. In this paper, a detailed analysis of the commutation aspects related to the diode rectifier of a brushless exciter of a 400*kVA* synchronous generator is presented and an accurate voltage drop prediction model is proposed and validated.**

***Index Terms*—Synchronous Generator, Excitation System, Diode Rectifier, Commutations.**

I. Introduction

It is well known that classical, field-wound, Synchronous Generators (SGs) consist of a stationary armature winding and a rotating field winding. The latter is fed by a DC current which traditionally is provided by using brushes and slip rings. In recent times, the utilization of this solution has seen a significant decrease, mainly because brushes can produce significant resistive voltage drops and need periodical maintenance and replacement. A more robust solution is that of providing the DC current by employing a brushless excitation system, consisting of a small "inside-out" electrical machine whose three phase output voltages are rectified by a rotating diode bridge and fed to the main generator's field winding, as presented in Fig.1.

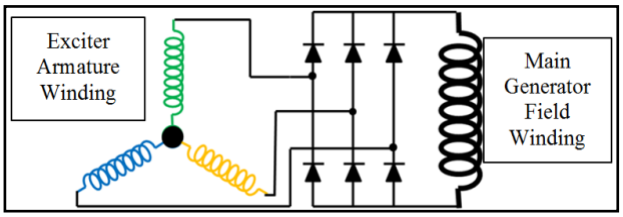

Fig. 1. Basic circuit of an exciter feeding into a three-phase bridge rectifier

The excitation system is a subpart of a more complex feedback control system, which includes the main synchronous machine and whose primary function is maintaining the output voltage constant at the stator terminals. This function is accomplished by controlling the output voltage of the exciter through control of the exciter field current. The field current is regulated by an Automatic Voltage Regulator (AVR), which is powered either by a permanent magnet generator (pilot exciter) in separately-excited systems or by the SG residual voltage in self-excited systems. An example of a brushless, self-excited, control system is shown in Fig. 2. Standard definitions of all the parts of a control excitation system are provided in [1].

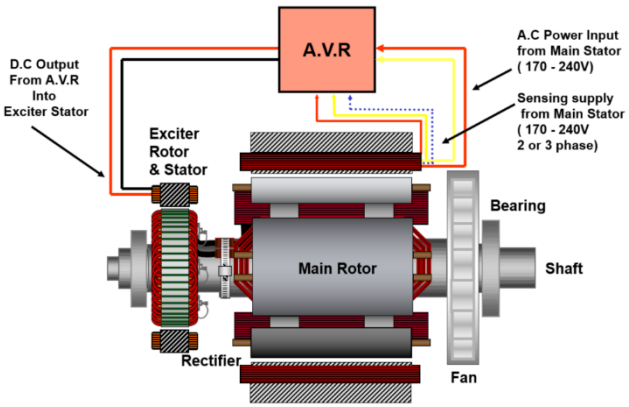

Fig. 2. Example of a brushless, self-excited, control system [Courtesy of Cummins Power Generation]

The electromagnetic design of an exciter is usually determined by the voltage and current requirements of the main SG at full-load rated condition [2, 3]. During the design stage, classical diode bridge theory [4] is usually used to convert between DC and AC quantities, where the commutations aspects are often neglected. However, for low to medium rated SGs, the exciter equivalent circuit's parameters can have a significant influence on the rectifier behavior. This indicates that the voltage drop due to the commutations needs to be taken into account also during the design stage, as it can have significant effects on the operation and efficiency of the entire system. In this paper, a detailed analysis of these aspects is presented and an accurate model for the prediction of the performance is proposed. In order to investigate this study, the exciter of a particular 400*kVA* SG is considered.

II. Analysis of the Commutation Processes in Diode Rectifiers

The excitation systems of large generating sets represent a very small part of the whole system (main generator, exciter, diode rectifier and AVR). For this reason, the main equivalent circuit's parameters of this electrical machine are often neglected and the bridge rectifier operation is considered ideal. In these conditions, if a three-phase system of alternating voltages is feeding the diode rectifier (Fig. 3), then at any instant in time, two diodes of different levels and legs conduct (e.g. V1 and V2). In simplistic terms, these are the diode with the most positive potential on its anode and that one with the most negative potential on its cathode.

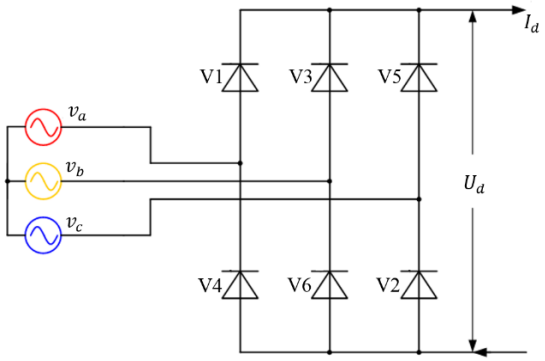

Fig. 3. Three phase, full wave, six-pulse bridge rectifier (ignoring the supply inductance)

If a DC current I_d is absorbed by a particular load, the currents on the AC side are ideally rectangular and their amplitudes are theoretically equal to I_d. The rectified voltage consists of n sinusoidal peaks per cycle (Fig. 4), where n is the number of diodes present in the AC/DC rectifier.

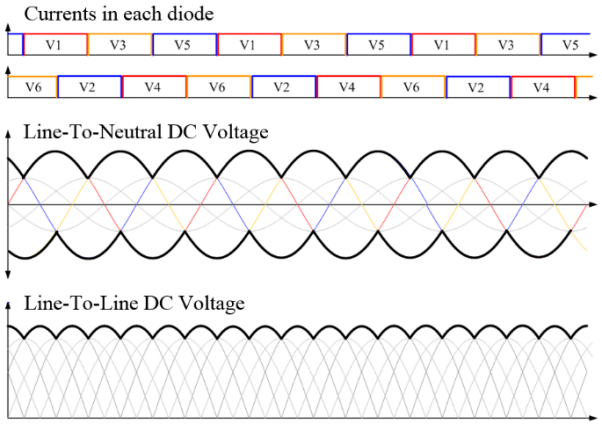

Fig. 4. Diode currents and rectified voltage in a six-pulse bridge rectifier (ignoring the supply inductance)

On the other hand, for low to medium rated SGs, the excitation system dimensions are comparable to those of the main generator. Hence, the exciter equivalent circuit's parameters may be no longer negligible. Thus, the inherent delay that the supply inductance creates in the diodes' commutations may become very important and can significantly affect the performance of the uncontrolled diode bridge. One of the more important aspects of this is the potential overlap in the conduction periods of the diodes. If the commutation takes less than (*1/n-th*) of one period, the process is called *simple commutation*. It the transfer process takes more than (*1/n-th*) of the period, then the operation mode is called *multiple commutation*. Besides these two modes of operation, it can occur that the commutation takes exactly (*1/n-th*) of one period. While these three commutation operating modes have been extensively dealt with in literature [5-9], they are 'lightly' introduced below in order to highlight their importance related to the voltage drop prediction in the excitation systems of SGs.

A. Operating Mode 1

Considering a six-pulse bridge, such as the one shown in Fig. 3 and assuming that

- all the diodes are ideal,
- the resistances of each phase are negligible,
- the current absorbed by the load is constant (DC),

then this operating mode can be studied by analyzing the commutation and conduction intervals over a 60° period. During commutation, two phases are short-circuited, say phases v_a and v_b. In this subinterval $i_1 + i_2 = I_d$ and the average load voltage is $U_d = \frac{1}{2}(v_a + v_b)$. During the conduction, the phase current is equal to the load current I_d and the load voltage is equal to the line-to-line voltage. Considering the above, the average DC load voltage U_d (Fig. 5) and the commutation angle μ can be derived and written as in (1) and (2).

$$U_d = \frac{V_{LL}\,3\sqrt{2}}{2\pi}(1 + \cos\ \mu) \tag{1}$$

$$\mu = a\cos\left(1 - \frac{2\omega L I_d}{V_{LL}\sqrt{2}}\right) \tag{2}$$

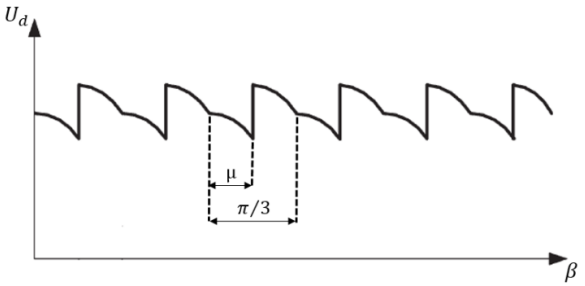

Fig. 5: Average DC voltage in operating mode 1

In (1) and (2), V_{LL} is the RMS value of the line-to-line voltage, ω the supply angular frequency and L the supply inductance.

B. Operating Mode 2

In this mode of operation, there are always three diodes conducting and the DC voltage is always $U_d = \frac{1}{2}(v_a + v_b)$. The overlapping angle μ is 60° and the commutation is spontaneously auto-delayed by an angle δ. Considering this, the average load voltage (Fig. 6) can be written as shown in (3) and an expression for δ is

given in (4).

$$U_d = \frac{V_{LL}\,3\sqrt{6}}{2\pi}\sin\left(\frac{\pi}{3} - \delta\right) \tag{3}$$

$$\delta = \frac{\pi}{3} - a\cos\left(\frac{2\omega LI_d}{V_{LL}\sqrt{2}}\right) \tag{4}$$

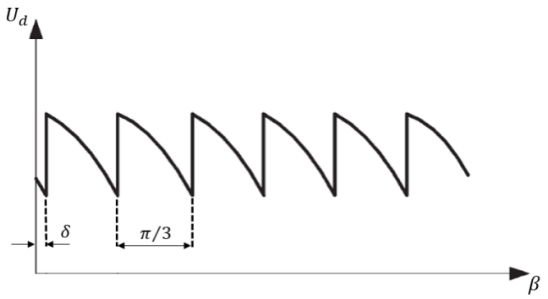

Fig. 6: Average DC voltage in operating mode 2

C. Operating Mode 3

When the load current I_d is so large that a delay of 30° is not sufficient to commutate the current within $(1/n-th)$ of a period, the commutation is termed as complex and/or multiple. Referring to Fig. 7,

- First, 2 simultaneous commutations occur in the subinterval t_1;
- Then only 1 commutation occurs during t_2;
- Finally, two commutations occur in the subinterval t_3.

During $t_1$andt_3, a three phase short circuit occurs and thus $i_1 + i_2 + i_3 = I_d$ and the DC voltage is of course null. During t_2, the load current and voltage behave as described in Section II.A. The final expression of the average load voltage (Fig. 7) is shown in (5) and the commutation angle is given in (6).

$$U_d = \frac{V_{LL}\,3\sqrt{6}}{2\pi}\left(1 + \cos\left(\mu + \frac{\pi}{3}\right)\right) \tag{5}$$

$$\mu = \frac{\pi}{3} - a\cos\left(1 - \frac{6\omega LI_d}{V_{LL}\sqrt{6}}\right) \tag{6}$$

D. Further Considerations

In the previous sections, it has been shown how the supply inductance can negatively affect the average value of the voltage rectified by an uncontrolled diode rectifier. The three typical operating modes of the rectifier have been recalled and the final expressions of the voltage on the DC bus have been shown in (1), (3) and (5). Also, the commutation angle's expressions have been provided in (2), (4) and (6), where it can be observed that, if I_d is maintained constant, the commutation angle can be reduced by

- Decreasing the supply angular frequency ω,
- Decreasing the supply inductance L,
- Increasing the supply AC voltage v_{LL}.

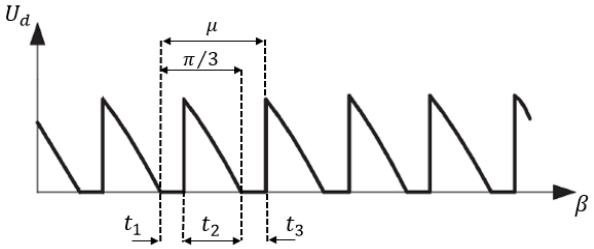

Fig. 7. Average DC voltage in operating mode 3

It is also important to show an expression for the voltage drop ΔV ensuing from the commutation processes, when for example the operating mode 1 occurs. This can be obtained by integrating the voltage drop due to the inductance over the commutation angle. Hence, for a six-pulse bridge rectifier, can be described by (7).

$$\Delta V = \frac{3\omega LI_d}{\pi} \tag{7}$$

Considering all the above, then it is clear that the supply inductance L, i.e. the phase inductance of the exciter, is a key parameter for determining the voltage drop. The models developed and used to estimate the machine inductance and the voltage drop are described in the following sections.

III. The Proposed Analytical Model

The brushless exciter under analysis is a 5.35kVA machine, with a 14 poles field winding placed on the stator and a three phase armature winding on the rotor. The exciter is designed to provide $\approx 5kW$ (DC) to the field winding of the main SG, when it operates at full-load condition. The machine is characterized by a low aspect ratio l/D (axial length/outer diameter), making its design quite compact. Considering the importance of accurately estimating the phase inductance of this small machine, then an analytical expression of the inductance matrix is developed based on the representation of a generic electrical machine, as given in (8).

$$L(\gamma) = l \cdot \int_0^{2\pi} \mu_E(\beta,\gamma)\cdot\overline{N}_E(\beta,\gamma)\cdot\overline{N}_E^{T}(\beta,\gamma)\cdot d\beta \tag{8}$$

The analytical derivation of (8) is entirely shown in [10] and is based on an equivalent-circuit-based approach. In (8), β is the rotor angular reference frame, γ is the mechanical variable associated with the rotor position, $\overline{N}_E(\beta,\gamma)$ the vector containing the equivalent Winding Functions (WFs) [12] of the machines' phases. The equivalent magnetic permeability function μ_E (β, γ) is given in (9), where μ_0 is the permeability of free space, r_{AG} (β, γ) is the air-gap radius and ε_{AG} (β, γ) the air-gap thickness, both evaluated along the tangential direction.

$$\mu_E(\beta,\gamma) = \mu_0\,\frac{r_{AG}(\beta,\gamma)}{\varepsilon_{AG}(\beta,\gamma)} \tag{9}$$

The main assumption behind (8) and (9) is the absence of saturation in the ferromagnetic materials. This allows one to consider the inductance *L(γ)* as only depending on the rotor position and not on the currents flowing in the machine windings. This hypothesis is justified for the application at hand as the exciters of SGs are designed for operating in linear conditions when the main machine operates at full-load. Another important assumption of the model is the neglecting of secondary phenomena, such as hysteresis and eddy currents.

Because of the intrinsic, structural symmetry that electrical machines present, it can be observed that the periodicity of the electrical quantities (i.e. $\overline{N}_E(\beta,\gamma)$) introduced in (8) is $2\pi/p$ (where p is the pole pair number), while the geometrical quantities shown in (9) have a periodicity which is instead half of that of the equivalent WFs. Considering this and referring to the approach shown in [10], all these functions can be developed in a Fourier series with respect to β. In particular, when a sinusoidal approximation is considered, only the mean values and the fundamental components are involved. Thus (8) can be developed into (10), where a single element of the machine inductance matrix is presented.

$$L_{ik}(\gamma) = \pi \cdot l \cdot {}^{1}N_i(\gamma) \cdot {}^{1}N_k(\gamma) \cdot \left\{ {}^{0}\mu_E \cdot \cos\left[p \cdot \left({}^{1}\beta_i(\gamma) - {}^{1}\beta_k(\gamma) \right) \right] + \frac{{}^{2}\mu_E}{2} \cdot \cos\left[p \cdot \left(2 \cdot {}^{2}\beta_E(\gamma) + {}^{1}\beta_i(\gamma) - {}^{1}\beta_k(\gamma) \right) \right] \right\} \quad (10)$$

In (10), ${}^{1}N_{i-k}(\gamma)$ and ${}^{1}\beta_{i-k}(\gamma)$ are the Fourier fundamental amplitudes and phases of the WFs of the *i-th* and *k-th* phase of the machine, respectively; ${}^{0}\mu_E$ is the mean value of the equivalent magnetic permeability function, while ${}^{2}\mu_E$ and ${}^{2}\beta_E(\gamma)$ are the second harmonic amplitude and phase of the same function, respectively. The second harmonic term ${}^{2}\mu_E$ is present only if the electrical machine is anisotropic.

All the above is then applied to the application at hand. A scheme of the machine exciter is shown in Fig. 8. In order to further the understanding of the under-investigation system, a simplified shape of the equivalent permeability function is shown in Fig. 9, with its second harmonic amplitude highlighted in red. In Fig. 10, the WF of the phase A is shown together with its fundamental component. It is important to note that the functions in Fig. 9 and 10 contain all the information necessary for the phase-A self-inductance calculation, namely the anisotropies present in the machine, the position of the active sides of the coil, the number of conductors per coil, etc.

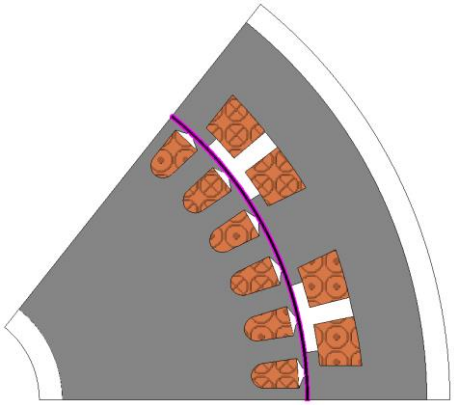

Fig. 8. 1 pole pair model of the 5.35*kVA* exciter.

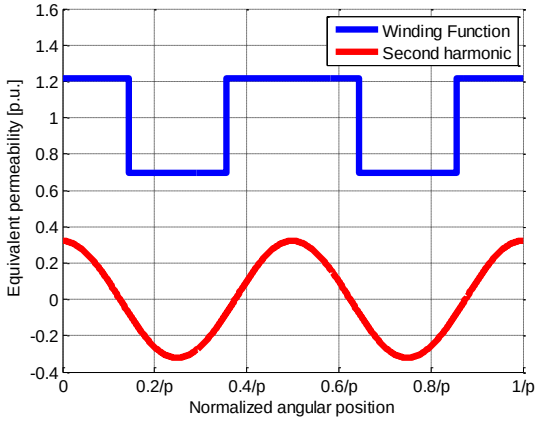

Fig. 9. Simplified equivalent permeability function.

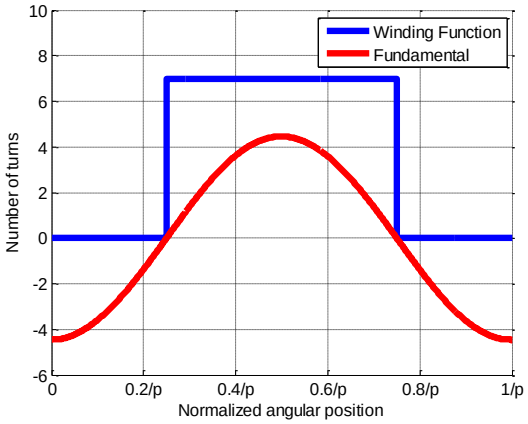

Fig. 10. Winding function of phase A.

Considering (10), then the main self-inductance of the phase A of the exciter can be calculated and this is shown in Fig. 11. Also, all the leakage inductances are calculated, according to the procedures described by [12]. These include:

- The airgap leakage inductance L_{ag};
- The slot leakage inductance L_{slot};
- The pole tip leakage inductance L_{pt};
- The end-winding leakage inductance L_{ew}.

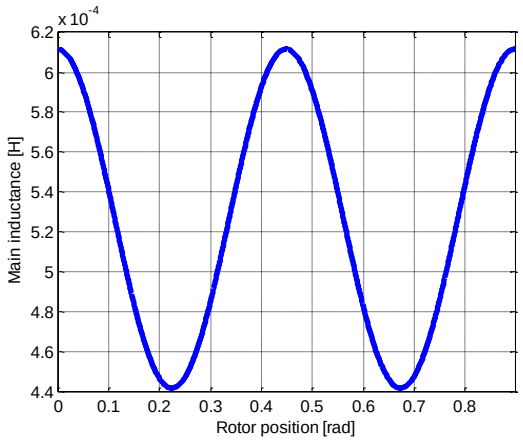

Fig. 11. A-phase main inductance as vs. rotor position.

The main inductance L_m shown in Fig. 11 and the calculated leakage inductances are then used in (11) to evaluate the voltage drop due to the commutation processes which occur in the diode rectifier of the brushless excitation system analyzed in this paper.

$$\Delta V = \frac{3\omega\left(L_m + L_{ag} + L_{slot} + L_{pt} + L_{ew}\right) I_d}{\pi} \quad (11)$$

The calculated value is ΔV=32.3V, which is about the 30% of the DC voltage needed by the rotor of the main SG when operating at full-load condition. The calculated ΔV can then be used to recalculate the exciter output AC voltage V_{LL_NEW} needed to compensate for it, as given in (12).

$$V_{LL\_new} = \frac{V_{LL} + \Delta V}{1.35} \quad (12)$$

The calculated inductance and the updated V_{LL_NEW} are then used in (2) to evaluate the commutation angle, resulting in $\mu \approx 58°$.

All the above confirm that the voltage drop to the commutations can be significantly large in low to medium rated SGs. In order to validate the analytical calculations of the inductance and the ensuing voltage drop, a 2-D Finite-Element (FE) model of the exciter is built. Details of this model and the analysis carried out on the exciter are given in the following section.

IV. FE Analysis of the Exciter

It is well known that an in-detail, FE analysis is more accurate than analytical approaches, especially when complex electromagnetic phenomena have to be accounted for [13]. Also, the commutation processes have to be considered for the sake of this study. Therefore, a 2-D FE model is built in order to achieve accurate results while minimizing the required computational resources (as opposed to a 3-D model). A number of circuital lumped resistances are coupled to the model to account for the end connections. To take advantage of the geometrical symmetries present in the machine, only (*1/7-th*) of the whole exciter is analyzed, as shown in Fig. 8. Test simulations are performed by coupling stator and rotor circuits to the FE model.

Considering all the above, static simulations have been carried out to calculate the inductances of the machine, according to the method described in [14]. This consists in evaluating the *d*- and *q*-axis inductances of the machine, allowing for the leakage inductances to be taken into account. Only the end-winding leakage inductance is not considered in the evaluation, as a 2-D FE model has been used for the analysis. The above-determined inductances are then used to evaluate the DC voltage drop ΔV. Furthermore, transient with motion simulations have been carried out in order to estimate the commutation angle μ and the rotor output voltage v_{LL} needed for maintaining the DC voltage and current on the main rotor at the desired values. The currents in two diodes during the conduction overlap are shown in Fig.12, highlighting the value of the commutation angle. Finally, a summary of the comparison between analytical and FE results is shown in Table I, where an excellent match can be observed.

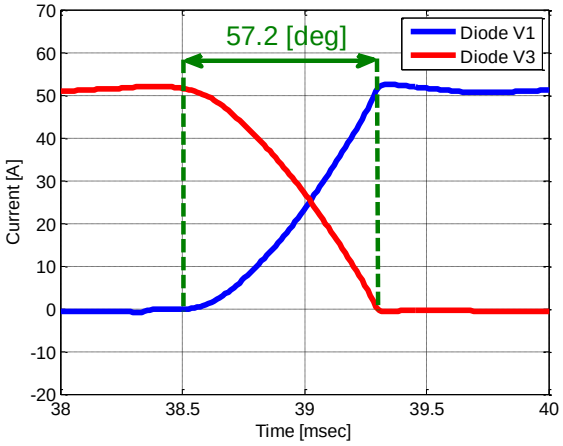

Fig. 12. Currents in 2 diodes during the commutation interval.

TABLE I
COMPARISON BETWEEN ANALYTICAL AND FE RESULTS

	Analytical	FE	Error
Phase Inductance	0.61H	0.59H	3.28%
Voltage Drop	32.3V	31.1V	3.72%
Commutation Angle	58.9°	57.2°	2.89%
Line-To-Line Voltage	101V	107V	5.61%

V. Experimental Results

In Table I, the proposed analytical model is compared to FE results, showing a very good similarity in terms of phase inductance. Analytical and FE results also confirm that the commutation processes cannot be neglected in the design of the particular exciter being analyzed in this paper. For the application at hand, a voltage drop equal to 30% of the DC voltage needed by the main rotor at full-load condition has been found. Having predicted the DC voltage reduction, then it is possible to estimate the real AC voltage value at which the exciter has to work to

provide the necessary power to the main rotor. This 'new' operating point has been again evaluated through the developed analytical and FE models. The results have been compared and successfully validated.

In order to further validate the FE model, the no-load FE characteristic of the 5.35*kVA* exciter is compared with available experimental results. This comparative exercise is shown in Fig. 13. In order to validate the 'new' estimated operating point, the value of the exciter field current, needed for providing the rated DC power to the main generator, was experimentally recorded. This value corresponds to V=108V on the experimental no-load characteristic (Fig. 13), showing again a very good match with analytical and FE results. A summary of this comparison is given in Table II.

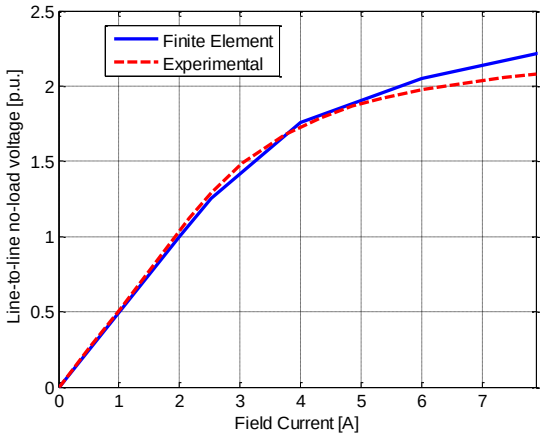

Fig. 13. No-Load Characteristics – Comparison.

TABLE II
ANALYTICAL, FE AND EXPERIMENTAL RESULTS COMPARISON OF THE NEW OPERATING POINT

----------	Analytical	FE	Experimental
Voltage	101V	107V	108V

VI. CONCLUSIONS

This paper deals with the analysis and prediction of the voltage drop produced by the diode commutation processes in the rotating diode bridge of small SGs. As vessel to expand the study, the work presented here was focused on a particular 5.35*kVA* brushless excitation system.

After having recalled some basics concepts related to the commutation phenomenon in diode rectifiers, an analytical model, based on the winding function method, was proposed and used to evaluate the machine phase inductance, which is critical for the evaluation of the voltage drop and the commutation angle. A FE model of the exciter under analysis was then built to validate the proposed method, with excellent similarity being achieved.

The method was then validated against experimental results. In Fig. 13 and Table II, an excellent match can be observed, illustrating the validity of the proposed analytical method. Special focus was given to the prediction of the new operating point at which the exciter has to work in order to compensate for the voltage drop due to the commutations.

The results obtained in this paper have confirmed that the commutation overlap cannot be neglected in excitation systems of low to medium rated SGs, such as a 400*kVA* alternator.

Considering all the above, it is clear that there is room for improvements in the design process of a brushless excitation system. In a future paper, the authors are developing an analytical and genetic-algorithm-based design tool aimed at minimizing the machine inductance and the ensuing voltage drop.

REFERENCES

[1] "IEEE Standard Definitions for Excitation Systems for Synchronous Machines", IEEE Std. 421.1, 1996 (revised 1996). "IEEE Guide for the Preparation of Excitation System Specifications", IEEE Std. 421.4, 1990.

[2] S. Khan, "Application Aspects of Generator and Excitation System for Process Plant", *IEEE Trans. Ind. Appl.*, vol. 35, no. 3, pp. 703-712, May/June1999.

[3] B. Wu, "Multipulse Diode Rectifiers", in *High-Power Converters and AC Drives*, USA: Wiley-IEEE Press, 2006, Ch. 3, pp. 35-64.

[4] M. Salameh and L. F. Kazda, "Analysis of the Steady State Performance of the Double Output Induction Generator," *IEEE Trans. Discussion Energy Cony.*, vol. EC-1, no. 1, March 1986, pp. 26-32.

[5] A.Sikora, B.Kulesz, "Influence of Diode Commutation Processes on Rectifier Tansformers Operation". *ICEM 2010 Proceedings* Rome, Italy

[6] W. J. Bonwick, "Characteristics of a Diode-Bridge-Loaded Synchronous Generator Without Damper Windings", *Proc. IEE*, Vol. 122, No.6, June 1975, pp 637-641

[7] Z. Ren, K. Yu, Q. Xin, and Y. Pan, "Performance of Homopolar Inductor Alternator With Diode-Bridge Rectifier and Capacitive Load," *IEEE Trans. Ind. Electron.*, vol. 60, no. 11, pp. 4891-4902, Nov.2013.

[8] M. A. Abdel-Halim and C. D. Manning, "Modeling a laminated brushless exciter-alternator unit in all modes of operation," *Proc. Inst. Elect. Eng. B*, vol. 138, no. 2, pp. 87–94, Mar. 1991.

[9] D. C. Aliprantis, S. D. Sudhoff, and B. T. Kuhn, "A brushless exciter model incorporating multiple rectifier modes and Preisach's hysteresis theory," *IEEE Trans. Energy Convers.*, vol. 21, no. 1, pp. 136–147, Mar. 2006

[10] P. Bolognesi, "A Mid-Complexity Analysis of Long-Drum-Type Electric Machines Suitable for Circuital Modelling", in *Proc. ICEM 2008 Conf.*, paper n. 99.

[11] A. Tessarolo, "Accurate computation of multiphase synchronous machine inductances based on winding function theory", *IEEE Trans. Energy Convers*., vol. 27, no. 4, pp. 895-904, Dec. 2012.

[12] Pyrhonen, J., Tapani, J., and Hrabovcovà, V. (2008). Design of Rotating Electrical Machines. Chicester, UK: John Wiley & Sons, Ltd.

[13] NuzzoS., GaleaM.,GeradaC., Gerada D., Mebarki A., Brown N. L.,"Damper Cage Loss Reduction and No-Load Voltage THD Improvements in Salient-Pole Synchronous Generators", *Proc. in Power Electronics, Machines and Drives(PEMD 2016), 8th IET International Conference on*., 2016.

[14] Bianchi, N., Electrical Machine Analysis Using Finite Elements. 2005: Crc